Modeling the diffusion of Na^+ in compacted water-saturated Na-bentonite as a function of pore water ionic strength

Ian C. Bourg[a,b,c,d,*], Garrison Sposito[a,c], Alain C.M. Bourg[b]

[a] *Civil and Environmental Engineering, University of California, Berkeley, CA 94720-1710, USA*

[b] *Environmental HydroGeochemistry, University of Pau, BP 1155, 64013 Pau Cedex, France*

[c] *Geochemistry Department, Lawrence Berkeley National Laboratory, Berkeley, CA 94720, USA*

[d] *ANDRA, 1/7 rue Jean Monnet, 92298 Châtenay-Malabry cedex, France*

* Corresponding author. Address: Ian C. Bourg, Hoffman Labs # 304, Harvard University, 20 Oxford Street, Cambridge, MA 02138, USA; email: ibourg@nature.berkeley.edu; tel: +1-510-701-2662; fax: +1-617-496-4387.

Abstract

Assessments of bentonite barrier performance in waste management scenarios require an accurate description of the diffusion of water and solutes through the barrier. A two-compartment macropore/nanopore model (on which smectite interlayer nanopores are treated as a distinct compartment of the overall pore space) was applied to describe the diffusion of $^{22}Na^{+}$ in compacted, water-saturated Na-bentonites and then compared with the well-known surface diffusion model. The two-compartment model successfully predicted the observed weak ionic strength dependence of the apparent diffusion coefficient (D_a) of Na^{+}, whereas the surface diffusion model did not, thus confirming previous research indicating the strong influence of interlayer nanopores on the properties of smectite clay barriers. Since bentonite mechanical properties and pore water chemistry have been described successfully with two-compartment models, the results in the present study represent an important contribution toward the construction of a comprehensive two-compartment model of compacted bentonite barriers.

Keywords: montmorillonite, smectite, bentonite, interlayer, nanopore, diffusion, adsorption, sodium.

1. Introduction

Bentonite clay barriers are extensively studied for use in the isolation of landfills (LaGrega et al., 2001; Jo et al., 2006; Lake et al., 2007) and in the containment of high-level radioactive waste stored in geological formations (Montes-H et al., 2005; Cleall et al., 2006; Samper et al., 2008). Because of the low hydraulic permeability of compacted water-saturated bentonite barriers, their performance strongly depends on the diffusion coefficients of water and solutes in such barriers (SKB, 2004; Montes-H et al., 2005). An emerging concept in the modeling of bentonite barrier properties is the explicit accounting for nanopores [nanometer-scale interlayer pores that make up more than half of the pore space in compacted water-saturated sodium-bentonite (Kozaki et al., 2001)] and macropores (all other pores) as two distinct "compartments" of the bentonite pore space (Hueckel et al., 2002; Bradbury and Baeyens, 2003; Ichikawa et al., 2004; Wersin et al., 2004; Jo et al., 2006; Xie et al., 2006; Bourg et al., 2006, 2007). Nanopore water has low thermodynamic activity (Torikai et al., 1996) and a low self-diffusion coefficient (Chang et al., 1995) and it is the main region of cation adsorption in compacted bentonite (Bradbury and Baeyens, 2003). Interpretation of measured diffusion coefficients with a model that explicitly distinguishes nanopores from macropores not only facilitates integration of diffusion data with two-compartment model interpretations of the chemical and mechanical properties of bentonite (Hueckel et al., 2002; Bradbury and Baeyens, 2003; Wersin et al., 2004), but also assists in the interpretation of spectroscopic and molecular dynamics simulation data on the behavior of water and solutes in smectite interlayers (Gay-Duchosal et al., 2000; Marry and Turq, 2003; Porion et al., 2007; Rotenberg et al., 2007; Kosakowski et al., 2008).

We have recently used the macropore/nanopore model to describe the relative apparent diffusion coefficients $D_{a,i}/D_0$ of water and cations (Na^+, Sr^{2+}) in compacted water-saturated bentonite (Bourg et al., 2006, 2007) with the equation:

$$\frac{D_{a,i}}{D_0} = \frac{1}{G_i}\left(\alpha_{\text{macropore}} + \alpha_{\text{interlayer}}\delta_{\text{interlayer}}\right) \qquad (1)$$

In equation 1, $D_{a,i}$ is a tracer diffusion coefficient of a species along the direction x_i, i.e., the ith diagonal element of the apparent diffusion coefficient tensor, $\mathbf{D_a}$; D_0 is the diffusion coefficient of the species in bulk liquid water; G_i (≥ 1) is a "geometry factor" that accounts for the influence of pore network geometry on $D_{a,i}$; $\delta_{\text{interlayer}}$ (≤ 1) is a "constrictivity factor" that accounts for the slower diffusion of the species of interest in nanopores relative to macropores or bulk water. The parameters $\alpha_{\text{macropore}}$ and $\alpha_{\text{interlayer}}$ are the mole fractions of the species of interest in macropores and nanopores, respectively; they are subject to the constraint $\alpha_{\text{macropore}} + \alpha_{\text{interlayer}} = 1$ if adsorption on montmorillonite edge surfaces or on non-montmorillonitic minerals is negligible.

In essence, equation 1 is a weighted sum of diffusive retardation factors for macropores ($1/G_i$) and nanopores ($\delta_{\text{interlayer}}/G_i$), with weighting being by the mole fraction of the species of interest in these two compartments. It is strictly valid only if the mass of montmorillonite per combined volume of montmorillonite and pore space, i.e., the partial montmorillonite dry density $\rho_{b,\text{mont}}$ (Liu et al., 2003; Sato and Suzuki, 2003), is greater than or equal to 0.98 kg dm^{-3}, the threshold value at which X-ray diffraction (XRD) reveals the existence of nanopores in Na-bentonite (Kozaki et al., 1998, 2001). Equation 1 also assumes that the two- and three-layer hydrates (observed by XRD in the range $0.98 < \rho_{b,\text{mont}} < 1.76$ kg dm^{-3}) and the external basal surfaces of montmorillonite stacks can be modeled as a single nanopore compartment (Bourg et al., 2007). For $0.2 < \rho_{b,\text{mont}} < 1.7$ kg dm^{-3} (i.e., ranging from a dilute montmorillonite gel to a compacted bentonite with most of its pore space located in nanopores), equation 1 accurately

predicts (1) the mean principal value of $\mathbf{D_a}$ for water tracers using a single fitting parameter [G = 4.0 ± 1.6, the average geometric factor along directions parallel and normal to bentonite compaction (Bourg et al., 2006)] and (2) the ratio $(D_{a,i}/D_0)_{cation}/(D_{a,i}/D_0)_{water}$ for sodium and strontium in Na-bentonite hydrated by low-ionic-strength solutions (where $\alpha_{macropore} \approx 0$ for cations) without the use of fitting parameters (Bourg et al., 2007).

In high-level radioactive waste repositories, pore water ionic strength I may be on the order of 0.3 to 0.6 mol dm^{-3} (Bradbury and Baeyens, 2003; Wersin et al., 2004) and the simplifying relation $\alpha_{macropore} \approx 0$ used by Bourg et al. (2007) may not be true. In the present paper, we model $^{22}Na^+$ diffusion in Na-bentonite for I = 0 to 1.0 mol dm^{-3} assuming that the isotope $^{22}Na^+$ and background Na^+ ions have the same affinity for montmorillonite surface adsorption sites. We are able to estimate the ionic strength dependence of $\alpha_{macropore}$ for $^{22}Na^+$ from simple charge-balance considerations. We also compare the macropore/nanopore model with the well-known surface diffusion model (Nye, 1979) in respect to experimental data on the apparent diffusion coefficient of sodium in compacted water-saturated Na-bentonite at ionic strengths I up to 1.0 mol dm^{-3} (Muurinen et al., 1990; Molera and Eriksen, 2002; Glaus et al., 2007; Kozaki et al., 2008).

2. Experimental database

Apparent diffusion coefficients of the trace isotope $^{22}Na^+$ in compacted water-saturated Na-bentonite as a function of background sodium electrolyte solution ionic strength (I) are reported by Muurinen et al. (1990), Molera and Eriksen (2002), Glaus et al. (2007) and Kozaki et al. (2008) (Fig. 1). These D_a-values were measured in one-dimensionally compacted bentonite, in the direction parallel to compaction ($x_{//}$), at constant and uniform temperature, background

106 electrolyte composition and macroscopic-scale bentonite properties. Experimental conditions are
107 summarized in Table 1.

108 In the through-diffusion method, a diffusion cell containing compacted water-saturated
109 Na-bentonite is placed in contact with two water reservoirs of equal sodium electrolyte
110 concentration (I), one of which is enriched with trace $^{22}Na^{+}$. The flux of $^{22}Na^{+}$ reaching the ^{22}Na-
111 depleted reservoir is monitored as a function of time and interpreted to obtain $D_{a,i}$ with the
112 relation $N_i = -D_{a,i}\, dC^*/dx_i$, where N_i is flux along the ith direction and C^* is mass of solute
113 (dissolved or adsorbed) per unit volume of porous medium (Muurinen et al., 1990; Molera and
114 Eriksen, 2002; Glaus et al., 2007). In the closed-cell method, blocks of compacted bentonite
115 hydrated by a sodium electrolyte solution of ionic strength I are placed on both sides of a thin
116 sample of ^{22}Na-enriched bentonite in a closed diffusion cell. After a chosen duration Δt the
117 bentonite sample is cut into slices and the observed concentration profile $C^*(x_i)$ of $^{22}Na^{+}$ is fitted
118 with an appropriate solution of the standard diffusion equation $dC^*/dt = D_{a,i}\, d^2C^*/dx_i^2$ to obtain
119 $D_{a,i}$ (Kozaki et al., 2008).

120 Confidence intervals for $\rho_{b,mont}$, estimated as described by Bourg (2004), account for errors
121 in the mass fraction of non-montmorillonitic solids ($1 - X_{mont}$), where X_{mont} is the mass fraction
122 of montmorillonite, and in the dry bulk density [the ρ_b values reported by Muurinen et al. (1990),
123 Molera and Eriksen (2002) and Kozaki et al. (2008) include about 2 ± 1 % water per unit mass of
124 Na-montmorillonite oven-dried at 373 K (Bourg, 2004)]. The error in reported I values was
125 assumed negligible, except for the experiments of Muurinen et al. (1990), where the dissolution
126 of readily-soluble minerals may have increased I by up to 0.025 mol dm^{-3} (Bourg, 2004).
127 Confidence intervals for $D_{a,i}$ were calculated as $\pm 2S/\sqrt{n}$, where S is the standard error of each
128 measured $D_{a,i}$ value [0.11 $D_{a,i}$ (Bourg, 2004)] and n is the number of replicates [$n = 2$ for the $D_{a,i}$

values reported by Kozaki et al. (2008) at $I \geq 0.05$ mol dm^{-3}; otherwise, $n = 1$]. Systematic errors in experimental $D_{a,i}$ data were assumed to cancel upon calculation of the ratio $(D_{a,i})_I/(D_{a,i})_{I=0}$ and, therefore, were neglected. [Glaus et al. (2007) reported much larger confidence intervals for $D_{a,i}$ at low ionic strengths. They calculated these confidence intervals from the errors of the effective diffusion coefficient D_e and rock capacity factor α ($D_a = D_e/\alpha$) but neglected the fact that the errors of D_e and α are strongly correlated for cationic solutes at low ionic strengths: for $^{22}Na^+$ at low I values, the porous plates that separate the clay sample and water reservoirs dominate the errors of D_e and α but should not affect the D_a values calculated with the "tracer profile analysis" method of Glaus et al. (2007).]

At high partial montmorillonite dry densities [$\rho_{b,mont} = 1.54 \pm 0.10$ (Muurinen et al., 1990; Molera and Eriksen, 2002) and 1.95 ± 0.05 kg dm^{-3} (Glaus et al., 2007)] $D_{a,i}$ values show little or no ionic strength dependence, whereas $D_{a,i}$ values at lower partial montmorillonite dry densities [$\rho_{b,mont} = 0.98 \pm 0.01$ kg dm^{-3} (Kozaki et al., 2008)] show significant ionic strength dependence (Fig. 1). This strong influence of $\rho_{b,mont}$ on the ionic strength dependence of $D_{a,i}$ values for cations in compacted bentonites appears not to have been noted previously.

3. Model predictions

The geometry factor $G_{//}$ for diffusion along the direction parallel to bentonite compaction ($x_{//}$) has not been measured, but may vary with $\rho_{b,mont}$ and X_{mont} (Kato et al., 1995; Bourg, 2004). To obviate this problem, we normalized all $D_{a,i}/D_0$ values to $D_{a,i}/D_0$ at $I \approx 0$ mol dm^{-3}, where $\alpha_{macropore} \approx 0$ for cations (Bourg et al., 2007), to obtain a relationship that does not contain $G_{//}$. If $\delta_{interlayer}$ and G_i are assumed independent of I, equation 1 yields:

151 $$\frac{\left(D_{\mathrm{a},i}\right)_I}{\left(D_{\mathrm{a},i}\right)_{I=0}} = \frac{\alpha_{\mathrm{macropore},I} + \alpha_{\mathrm{interlayer},I}\delta_{\mathrm{interlayer}}}{\delta_{\mathrm{interlayer}}} \qquad (2)$$

152 For sodium, $\delta_{\mathrm{interlayer}} = 0.32 \pm 0.06$ and $\alpha_{\mathrm{macropore},I} + \alpha_{\mathrm{interlayer},I} = 1$ (Bourg et al., 2007). If positive
153 anion adsorption in the interlayer is negligible and if $^{22}Na^+$ and the background Na^+ ions have the
154 same affinity for the montmorillonite surface, the mole fraction $\alpha_{\mathrm{interlayer}}$ for $^{22}Na^+$ in Na-
155 bentonite can be calculated from a simple charge balance consideration:

156 $$\alpha_{\mathrm{interlayer},I} = \frac{\sigma_{0,\mathrm{mont}}\rho_{\mathrm{b,mont}}}{\sigma_{0,\mathrm{mont}}\rho_{\mathrm{b,mont}} + I\left(1 - f_{\mathrm{interlayer}}\right)\left(1 - \frac{\rho_{\mathrm{b,mont}}}{\rho_{\mathrm{mont}}}\right)} \qquad (3)$$

157 In equation 3, $\sigma_{0,\mathrm{mont}}$ and ρ_{mont} are respectively the specific structural charge (Table 1) and the
158 mass density (2.84 ± 0.04 kg dm^{-3}) of montmorillonite lamellae and $f_{\mathrm{interlayer}}$, the volume fraction
159 of bentonite pore space located in nanopores, can be estimated from XRD measurements of the
160 interlayer spacing in compacted bentonite (Bourg et al., 2006).

161 By contrast, on the surface diffusion model, $D_{\mathrm{a},i}$ for cations is expressed as the weighted
162 sum of diffusive retardation terms for free ($1/G_i$) and adsorbed cations ($1/G_i \times D_s/D_0$, where D_s is
163 a surface diffusion coefficient), with weighting by the mole fractions of free and adsorbed
164 cations (Nye, 1979; Jensen and Radke, 1988; Molera and Eriksen, 2002):

165 $$\frac{D_{\mathrm{a},i}}{D_0} = \frac{1}{G_i}\frac{\varepsilon + \rho_{\mathrm{b}}K_{\mathrm{d}}\left(\frac{D_{\mathrm{s}}}{D_0}\right)}{\varepsilon + \rho_{\mathrm{b}}K_{\mathrm{d}}} \qquad (4)$$

166 In equation 4, ε and ρ_b are respectively the porosity and dry bulk density of the porous medium
167 and K_d is the distribution coefficient for the cation ($K_d = q/C$, if q is the amount adsorbed per
168 mass of solid and C is the amount in solution per volume of pore water). Using the simplifying
169 relation $D_s/D_0 \approx \delta_{\mathrm{interlayer}}$ (Bourg et al., 2007) and normalizing all $D_{a,i}/D_0$ values to $D_{a,i}/D_0$ at $I \approx 0$
170 mol dm^{-3} (where $\rho_b K_d >> \varepsilon$), we obtain the surface diffusion model prediction of $(D_{a,i})_I/(D_{a,i})_{I=0}$:

171 $$\frac{(D_{a,i})_I}{(D_{a,i})_{I=0}} = \frac{\varepsilon + \rho_b K_d \delta_{interlayer}}{(\varepsilon + \rho_b K_d)\delta_{interlayer}} \qquad (5)$$

172 Equation 5 would be formally identical to equation 2 if the mole fractions of free and adsorbed
173 cations, $\alpha_{free} = \varepsilon/(\varepsilon + \rho_b K_d)$ and $\alpha_{adsorbed} = \rho_b K_d/(\varepsilon + \rho_b K_d)$, in the surface diffusion model were
174 equal to the mole fractions of macropore and nanopore cations, $\alpha_{macropore}$ and $\alpha_{interlayer}$, in the
175 macropore/nanopore model. Charge balance considerations similar to those used to obtain
176 equation 3 yield an expression for the distribution coefficient:

177 $$K_d = \frac{\sigma_{0,mont} X_{mont}}{I} \qquad (6)$$

178 Equations 2 and 5 yield respectively macropore/nanopore and surface diffusion model
179 predictions of $(D_{a,i})_I/(D_{a,i})_{I=0}$ which can be tested, without fitting parameters, against the
180 experimental data of Muurinen et al. (1990), Molera and Eriksen (2002), Glaus et al. (2007) and
181 Kozaki et al. (2008).

182

183 **4. Results and discussion**

184 Model predictions of the ionic strength dependence of $(D_{a,i})_I/(D_{a,i})_{I=0}$ based on $\delta_{interlayer} = 0.32 \pm$
185 0.06 (Bourg et al., 2007), $\rho_{mont} = 2.84 \pm 0.04$ kg dm^{-3} (Bourg, 2004), $f_{interlayer}$ values estimated as
186 in Bourg et al. (2006), and $\sigma_{0,mont}$, X_{mont}, ρ_b, $\rho_{b,mont}$, and ε values compiled in Table 1 are
187 compared with experimental data in Fig. 2. The macropore/nanopore model is consistent with all
188 available experimental data on the ionic strength dependence of $^{22}Na^+$ diffusion in compacted
189 water-saturated Na-bentonite, whereas the surface diffusion model overestimates the ionic-
190 strength-dependence of the sodium D_a values in MX-80 bentonite at $\rho_{b,mont} = 1.54 \pm 0.10$ kg dm^{-3}
191 (Fig. 2b). Bourg et al. (2007) also found that the macropore/nanopore model is consistent with

192 the dependence of sodium and strontium diffusion on $\rho_{b,mont}$ in compacted water-saturated Na-
193 bentonite, whereas the surface diffusion model is not.

194 Overall, the macropore/nanopore model predicts a weaker ionic strength dependence of
195 sodium D_a than does the surface diffusion model. At $\rho_{b,mont} = 0.98$ kg dm^{-3}, the lowest value at
196 which the macropore/nanopore model is strictly applicable, the ionic strength dependence of D_a
197 it predicts is about half of that predicted by the surface diffusion model. At $\rho_{b,mont} \geq 1.72$ kg dm^{-3},
198 all pore water is located in nanopores and the macropore/nanopore model predicts no ionic
199 strength dependence of sodium D_a, whereas the surface diffusion model still predicts a
200 significant ionic strength dependence. These differences can be readily understood by
201 examining the situation at $\rho_{b,mont} = 1.72$ kg dm^{-3} ($f_{interlayer} \approx 1$), wherein all sodium cations are
202 located in nanopores ($\alpha_{macropore} = 0$) and the macropore/nanopore model therefore predicts that
203 $D_{a,i}$ must be independent of I. In the same situation, however, a non-negligible fraction of the
204 interlayer cations is free (i.e., non-adsorbed), and this free sodium fraction, $\alpha_{free} = \varepsilon/(\varepsilon + \rho_b K_d) >$
205 0, in fact increases with ionic strength. The surface diffusion model assumes that free species are
206 retarded only by geometric effects and, therefore, it predicts that $D_{a,i}$ increases with I even when
207 all cations are forced to diffuse through nanopores.

208 Beyond the evident benefit for understanding diffusion in bentonite barriers at pore scales,
209 our results have two notable implications for the modeling of bentonite barrier properties.
210 Firstly, a weak ionic strength dependence of sodium D_a values implies that bentonite barrier
211 performance will be relatively insensitive to pore water ionic strength, which is particularly
212 desirable in performance assessment if this latter property of the bentonite barrier is not well
213 known. Secondly, since bentonite mechanical properties and pore water chemistry have been
214 described successfully with two-compartment models (Hueckel et al., 2002; Bradbury and

215 Baeyens, 2003; Wersin et al., 2004), the success of the macropore/nanopore diffusion model is
216 an important step toward the construction of a comprehensive two-compartment model of
217 bentonite pore water chemistry, mechanical properties, and water and solute diffusion.
218 The diffusion of sodium in Na-bentonite can be modeled with equation 2 because the value
219 of $\alpha_{interlayer}$ for $^{22}Na^+$ in Na-bentonite can be estimated from simple charge-balance considerations
220 (equation 3). For cations other than sodium, estimation of $\alpha_{interlayer}$ will require knowledge of the
221 selectivity coefficient for the cation exchange reaction:
222 $$z\mathrm{Na}^+_{\mathrm{interlayer}} + C^{z+}_{\mathrm{macropore}} \Leftrightarrow z\mathrm{Na}^+_{\mathrm{macropore}} + C^{z+}_{\mathrm{interlayer}} \qquad (7)$$
223 where C^{z+} is the competing cation. Unfortunately, reliable experimental data on the
224 macropore/nanopore partitioning of cations in compacted bentonite are very scarce. For
225 example, cesium adsorption in compacted bentonite has been reported as either weaker than
226 (Oscarson et al., 1994), equal to (Suzuki et al., 2007), or stronger than (Molera and Eriksen,
227 2002; Van Loon and Glaus, 2008) that in bentonite aqueous suspensions. Thus further research
228 on cation adsorption in compacted bentonite will be required before equation 2 can predict the
229 ionic strength dependence of the D_a values for cations other than Na^+.
230 We should note also that the macropore-nanopore model prediction in Fig. 2c is not strictly
231 derived from equation 1, since this latter equation is valid only in the range $\rho_{b,mont}$ = 0.98 to 1.72
232 kg dm^{-3} where the interlayer nanopore compartment is composed of 2- and 3-layer hydrates
233 (Bourg et al., 2006, 2007). Compaction to $\rho_{b,mont}$ > 1.72 kg dm^{-3} causes the disappearance of the
234 macropore compartment and requires the existence of a 1-layer hydrate "subcompartment" of the
235 nanopore compartment (Bourg et al., 2006). Molecular dynamics simulations (Chang et al.,
236 1995; Kosakowski et al., 2008) imply that the constrictivity factor of sodium in montmorillonite
237 1-layer hydrates ($\delta_{1\text{-layer}}$) is significantly lower than in 2- and 3-layer hydrates ($\delta_{interlayer}$). At

238 $\rho_{b,mont} > 1.72$ kg dm^{-3}, equation 1 can be rewritten to account for the absence of macropores and

239 the existence of a 1-layer hydrate subcompartment:

240 $$\frac{D_{a,i}}{D_0} = \frac{1}{G_i}\left(\alpha_{interlayer}\delta_{interlayer} + \alpha_{1\text{-}layer}\delta_{1\text{-}layer}\right) \qquad (8)$$

241 Dividing $D_{a,i}/D_0$ in equation 8 by its value at $I \approx 0$ mol dm^{-3} and using the fact that the

242 partitioning of $^{22}Na^+$ between the 1-layer hydrate and other nanopores is independent of I, we

243 find from equation 8 that $(D_{a,i})_I/(D_{a,i})_{I=0} = 1$ at $\rho_{b,mont} > 1.72$ kg dm^{-3}. This result, which is

244 identical to that obtained with equation 2 at $\rho_{b,mont} = 1.72$ kg dm^{-3}, is shown in Fig. 2c.

245

246 **5. Summary**

247 The macropore/nanopore model of water and solute diffusion in compacted water-saturated

248 bentonite describes all available data on the ionic strength dependence of sodium D_a values in

249 Na-bentonite, whereas the surface diffusion model does not. This result—along with our

250 previous finding that the macropore/nanopore model correctly predicts the dependence of water,

251 sodium and strontium D_a values on $\rho_{b,mont}$ (Bourg et al., 2006, 2007)—demonstrates that the

252 macropore/nanopore model is a useful tool for characterizing diffusion in bentonite barriers. The

253 weak ionic strength dependence of sodium D_a values predicted by the macropore/nanopore

254 model indicates that bentonite barrier performance is less sensitive to pore water ionic strength

255 than suggested previously by the surface diffusion model. Use of the macropore/nanopore model

256 to predict the ionic strength dependence of D_a for cations other than sodium, however, will

257 require improved knowledge of the selectivity coefficients for the partitioning of cations between

258 macropore and interlayer nanopore compartments in compacted bentonite.

259

260 **Acknowledgements**

The lead author (ICB) is grateful for a predoctoral fellowship from the French Agency for Radioactive Waste Management (ANDRA, Agence Nationale pour la Gestion des Déchets Radioactifs, Châtenay-Malabry, France). The data analysis reported in this paper also was supported in part by the Director, Office of Energy Research, Office of Basic Energy Sciences, of the US Department of Energy under Contract No. DE-AC02-05CH11231. The interpretation of experimental diffusion data benefited greatly from discussions between the first author and Professor T. Kozaki, Hokkaido University (Japan).

References

Bourg, I.C., 2004. Diffusion of water and inorganic ions in saturated compacted bentonite, Ph.D. Thesis, University of California: Berkeley.

Bourg, I.C., Sposito, G., Bourg, A.C.M., 2006. Tracer diffusion in compacted, water-saturated bentonite. Clays Clay Miner. 54, 363-374.

Bourg, I.C., Sposito, G., Bourg, A.C.M., 2007. Modeling cation diffusion in compacted water-saturated sodium bentonite at low ionic strength. Environ. Sci. Technol. 41, 8118-8122.

Bradbury, M.H., Baeyens, B., 1997. A mechanistic description of Ni and Zn sorption on Na-montmorillonite. Part II: modelling. J. Contam. Hydrol. 27, 223-248.

Bradbury, M.H., Baeyens, B., 2003. Porewater chemistry in compacted re-saturated MX-80 bentonite. J. Contam. Hydrol. 61, 329-338.

Chang, F.-R.C., Skipper, N.T., Sposito, G., 1995. Computer simulation of interlayer molecular structure in sodium montmorillonite hydrates. Langmuir 11, 2734-2741.

Cleall, P.J., Melhuish, T.A., Thomas, H.R., 2006. Modelling the three-dimensional behaviour of a prototype nuclear waste repository. Eng. Geol. 85, 212-220.

284 Gay-Duchosal, M., Powell, D.H., Lechner, R.E., Rufflé, B., 2000. QINS studies of water
285 diffusion in Na-montmorillonite. Physica B 276/278, 234-235.
286 Glaus, M.A., Baeyens, B., Bradbury, M.H., Jakob, A., Van Loon, L.R., Yaroshchuk, A., 2007.
287 Diffusion of ^{22}Na and ^{85}Sr in montmorillonite: Evidence of interlayer diffusion being the
288 dominant pathway at high compaction. Environ. Sci. Technol. 41, 478-485.
289 Hueckel, T., Loret, B., Gajo, A., 2002. Expansive clays as two-phase, deformable reactive
290 continua: Concepts and modeling options. In: Di Maio, C., Hueckel, T., Loret, B. (Eds.),
291 Chemo-Mechanical Coupling in Clays, Balkema Publ.: Lisse, pp. 105-120.
292 Ichikawa, Y., Kawamura, K., Fujii, N., Kitayama, K., 2004. Microstructure and micro/macro-
293 diffusion behavior of tritium in bentonite. Appl. Clay Sci. 26, 75-90.
294 Jensen, D.J., Radke, C.J., 1988. Caesium and strontium diffusion through sodium
295 montmorillonite at elevated temperature. J. Soil Sci. 39, 53-64.
296 Jo, H.Y., Benson, C.H., Edil, T.B., 2006. Rate-limited cation exchange in thin bentonitic barrier
297 layers. Can. Geotech. J. 43, 370-391.
298 Kato, H., Muroi, M., Yamada, N., Ishida, H., Sato, H. Estimation of effective diffusivity in
299 compacted bentonite. In: Murakami, T., Ewing, R.C. (Eds.), Scientific Basis for Nuclear
300 Waste Management XVIII, Materials Research Society, Pittsburgh, pp. 277-284.
301 Kosakowski, G., Churakov, S.V., Thoenen, T., 2008. Diffusion of Na and Cs in montmorillonite.
302 Clays Clay Miner. 56, 190-206.
303 Kozaki, T., Fujishima, A., Sato, S., Ohashi, H., 1998. Self-diffusion of sodium ions in compacted
304 sodium montmorillonite. Nucl. Technol. 121, 63-69.
305 Kozaki, T., Inada, K., Sato, S., Ohashi, H., 2001. Diffusion mechanism of chloride ions in
306 sodium montmorillonite. J. Contam. Hydrol. 47, 159-170.

Kozaki, T., Liu, J., Sato, S., 2008. Diffusion mechanism of sodium ions in compacted montmorillonite under different NaCl concentration. Phys. Chem. Earth, in press (doi:10.1016/j.pce.2008.05.007).

LaGrega, M.D., Buckingham, P.L., Evans, J.C., 2001. Hazardous Waste Management, 2nd Ed., McGraw-Hill: Boston.

Lake, C.B., Cardenas, G., Goreham, V., Gagnon, G.A., 2007. Aluminium migration through a geosynthetic clay liner. Geosynthetics International 14, 201-210.

Liu, J., Kozaki, T., Horiuchi, Y., Sato, S., 2003. Microstructure of montmorillonite/silica sand mixture and its effects on the diffusion of strontium ions. Applied Clay Sci. 23, 89-95.

Marry, V., Turq, P., 2003. Microscopic simulations of interlayer structure and dynamics in bihydrated heteroionic montmorillonites. J. Phys. Chem. B 107, 1832-1839.

Molera, M., Eriksen, T., 2002. Diffusion of $^{22}Na^{+}$, $^{85}Sr^{2+}$, $^{134}Cs^{+}$ and $^{57}Co^{2+}$ in bentonite clay compacted to different densities: experiments in modeling. Radiochim. Acta 90, 753-760.

Montes-H, G., Marty, N., Fritz, B., Clement, A., Michau, N., 2005. Modelling of long-term diffusion-reaction in a bentonite barrier for radioactive waste confinement. Appl. Clay Sci. 30, 181-198.

Muurinen, A., Olin, M., Uusheimo, K., 1990. Diffusion of sodium and copper in compacted sodium bentonite at room temperature. In: Oversby, V.M., Brown, P.W. (Eds.), Scientific Basis for Nuclear Waste Management XIII, Materials Research Society, Pittsburgh, pp. 641-647.

Nye, P.H., 1979. Diffusion of ions and uncharged solutes in soils and soil clays. Adv. Agron. 31, 225-272.

329 Ochs, M., Lothenbach, B., Shibata, M., Sato, H., Yui, M., 2003. Sensitivity analysis of
330 radionuclide migration in compacted bentonite: a mechanistic model approach. J. Contam.
331 Hydrol. 61, 313-328.
332 Oscarson, D.W., Hume, H.B., King, F., 1994. Sorption of cesium on compacted bentonite. Clays
333 Clay Miner. 42, 731-736.
334 Porion, P., Michot, L.J., Faugère, A.M., Delville, A., 2007. Influence of confinement on the
335 long-range mobility of water molecules within clay aggregates: A ^{2}H NMR analysis using
336 spin-locking relaxation rates. J. Phys. Chem. C 111, 13117-13128.
337 Rotenberg, B., Marry, V., Vuilleumier, R., Malikova, N., Simon, C.,Turq, P., 2007. Water and
338 ions in clays: Unraveling the interlayer/micropore exchange using molecular dynamics.
339 Geochim. Cosmochim. Acta 71, 5089-5101.
340 Samper, J., Zheng, L., Montenegro, L., Fernández, A.M., Rivas, P., 2008. Coupled thermo-
341 hydro-chemical models of compacted bentonite after FEBEX *in situ* test. Applied Geochem.
342 23, 1186-1201.
343 Sato, H., Suzuki, S., 2003. Fundamental study on the effect of an orientation of clay particles on
344 diffusion pathway in compacted bentonite. Applied Clay Sci. 23, 51-60.
345 Suzuki, S., Haginuma, M., Suzuki, K., 2007. Study of sorption and diffusion of ^{137}Cs in
346 compacted bentonite saturated with saline water at 60°C, J. Nucl. Sci. Technol. 44, 81-89.
347 Torikai, Y., Sato, S., Ohashi, H., 1996. Thermodynamic properties of water in compacted
348 sodium montmorillonite. Nucl. Technol. 115, 73-80.
349 Van Loon, L.R., Glaus, M.A., 2008. Mechanical compaction of smectite clays increases ion
350 exchange selectivity for cesium. Environ. Sci. Technol. 42, 1600-1604.

Wersin, P., Curti, E., Appelo, C.A.J., 2004. Modelling bentonite-water interactions at high solid/liquid ratios: swelling and diffuse double layer effects. Appl. Clay Sci. 26, 249-257.

Xie, M., Bauer, S., Kolditz, O., Nowak, T., Shao, H., 2006. Numerical simulation of reactive processes in an experiment with partially saturated bentonite. J. Contam. Hydrol. 83, 122-147.

Table 1. Experimental conditions of reported measurements of $^{22}Na^{+}$ diffusion in compacted water-saturated Na-bentonite as a function of ionic strength.

	Muurinen et al. (1990), Molera and Eriksen (2002)	Glaus et al. (2007)	Kozaki et al. (2008)
Method	through-diffusion	through-diffusion	closed-cell
Solid	MX-80 bentonite	Montmorillonite from Milos (Greece)	purified Kunipia-F bentonite
$\sigma_{0,mont}$ (mol_c kg^{-1})[a]	0.88 ± 0.088	0.8 ± 0.08	1.08 ± 0.108
X_{mont} (-)	0.725 ± 0.075	1.0	1.0
ρ_b (kg dm^{-3})	1.76 ± 0.01	1.95 ± 0.05	0.98 ± 0.01
$\rho_{b,mont}$ (kg dm^{-3})	1.54 ± 0.10	1.95 ± 0.05	0.98 ± 0.01
ε (-)[b]	0.380 ± 0.009	0.313 ± 0.020	0.655 ± 0.006
I (mol dm^{-3})	0.014 ± 0.012, 0.05, 0.1, 1.0	0.01, 0.1, 0.5, 0.7, 1.0	0.00, 0.05, 0.1, 0.2, 0.4, 0.5

[a] $\sigma_{0,mont}$ was assumed equal to the cation-exchange capacity (CEC) of the montmorillonite fraction as reported by Baeyens and Bradbury (1997), Glaus et al. (2007) and Ochs et al. (2003); confidence intervals were assigned a typical value of ± 10%.

[b] Porosity was estimated with the relation $\varepsilon = (1 - \rho_b/\rho_{mont})$, where the density of non-montmorillonitic minerals is assumed similar to that of montmorillonite (ρ_{mont} = 2.84 ± 0.04 kg dm^{-3}).

List of Figures

Fig. 1. Apparent diffusion coefficient $D_{a,//}$ of sodium in one-dimensionally compacted water-saturated Na-bentonite at 298 K, plotted as a function of background ionic strength I. Data were measured at $\rho_{b,mont}$ = 0.98 ± 0.01 (Kozaki et al., 2008), 1.54 ± 0.10 (Muurinen et al., 1990; Molera and Eriksen, 2002) and 1.95 ± 0.05 kg dm^{-3} (Glaus et al., 2007).

Fig. 2. Apparent diffusion coefficient $D_{a,//}$ of sodium in one-dimensionally compacted water-saturated Na-bentonite normalized to its value at I = 0, plotted as a function of background ionic strength I at $\rho_{b,mont}$ = 0.98 ± 0.01 (Fig. 2a), 1.54 ± 0.10 (Fig. 2b) and 1.95 ± 0.05 kg dm^{-3} (Fig. 2c). Experimental data are compared with predictions obtained with the surface diffusion and macropore/nanopore models (solid lines, with confidence intervals shown as dashed lines). In each figure the upper and lower sets of lines (blue and thick brown lines, respectively) correspond to surface diffusion and macropore/nanopore model predictions. At $\rho_{b,mont} \geq$ 1.72 kg dm^{-3}, the macropore/nanopore model predicts $(D_{a,//})_I/(D_{a,//})_{I=0}$ = 1 (Fig. 1c).

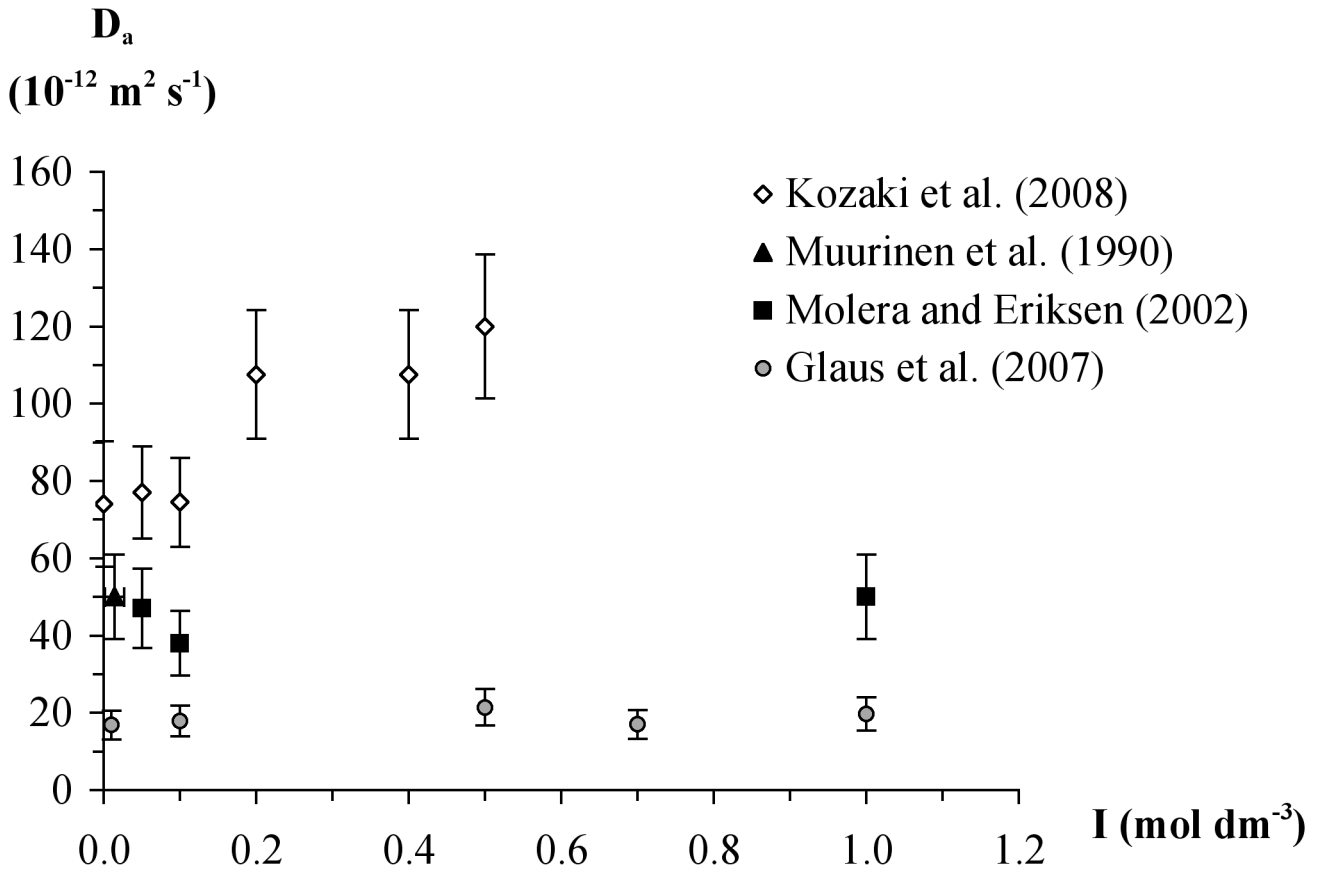
D_a
$(10^{-12}\ m^2\ s^{-1})$
160
140
120
100
80
60
40
20
0
0.0
0.2
0.4
0.6
0.8
1.0
1.2
I (mol dm^{-3})
Kozaki et al. (2008)
Muurinen et al. (1990)
Molera and Eriksen (2002)
Glaus et al. (2007)

a)

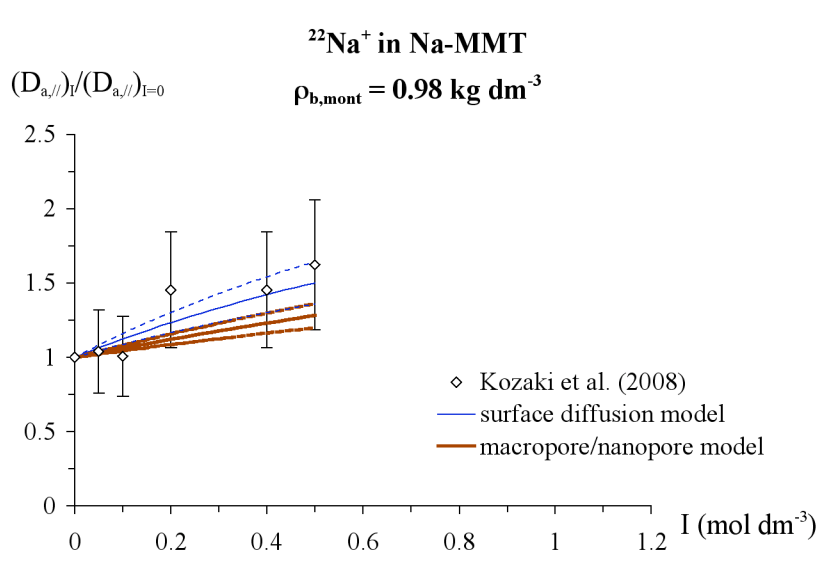
$^{22}Na^+$ in Na-MMT
$\rho_{b,mont}$ = 0.98 kg dm^{-3}
$(D_{a,//})_I/(D_{a,//})_{I=0}$
Kozaki et al. (2008)
surface diffusion model
macropore/nanopore model
I (mol dm^{-3})

b)

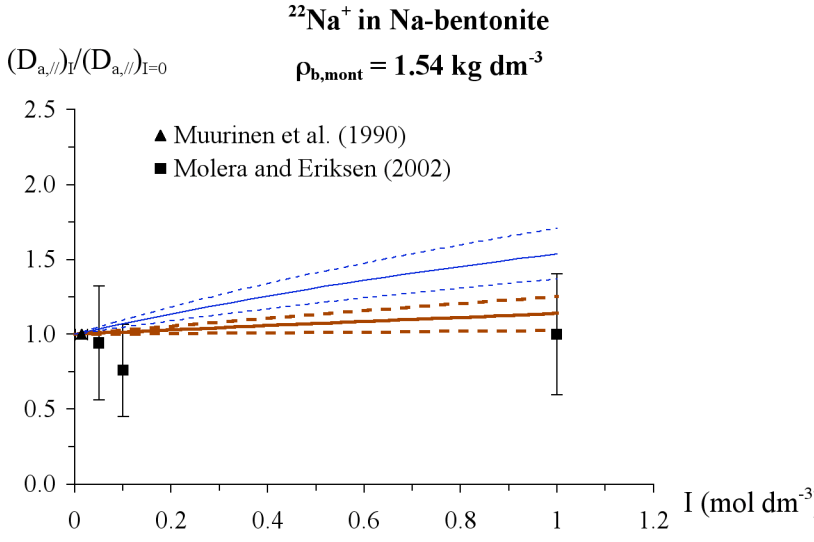
$^{22}Na^+$ in Na-bentonite
$\rho_{b,mont}$ = 1.54 kg dm^{-3}
$(D_{a,//})_I/(D_{a,//})_{I=0}$
Muurinen et al. (1990)
Molera and Eriksen (2002)
I (mol dm^{-3})

c)

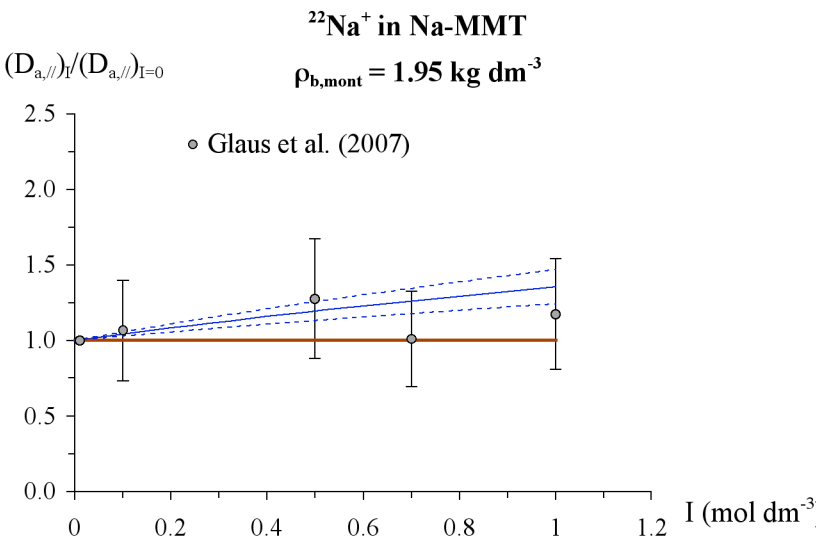
$^{22}Na^+$ in Na-MMT
$\rho_{b,mont}$ = 1.95 kg dm^{-3}
$(D_{a,//})_I/(D_{a,//})_{I=0}$
Glaus et al. (2007)
I (mol dm^{-3})